

# Commissioning status of Subaru laser guide star adaptive optics system

Yutaka Hayano<sup>a</sup>, Hideki Takami<sup>a</sup>, Shin Oya<sup>a</sup>, Masayuki Hattori<sup>a</sup>, Yoshihiko Saito<sup>a</sup>, Makoto Watanabe<sup>b</sup>, Olivier Guyon<sup>a,c</sup>, Yosuke Minowa<sup>a</sup>, Sebastian E. Egner<sup>a</sup>, Meguru Ito<sup>a</sup>, Vincent Garrel<sup>a</sup>, Stephen Colley<sup>a</sup>, Taras Golota<sup>a</sup>, Masanori Iye<sup>d</sup>

<sup>a</sup>Subaru Telescope, National Astronomical Observatory of Japan, 650 North A'ohoku Place, Hilo, HI, USA 96720;

<sup>b</sup>Department of Cosmosciences, Graduate School of Science, Hokkaido University, Kita-10, Nishi-8, Kita-ku, Sapporo, Japan 060-0810;

<sup>c</sup>Department of Astronomy/Steward Observatory, University of Arizona, 933 North Cherry Avenue, Tucson, AZ 85721-0065;

<sup>d</sup>National Astronomical Observatory of Japan, 2-21 Osawa, Mitaka, Tokyo, Japan 181-8588

## ABSTRACT

The current status of commissioning and recent results in performance of Subaru laser guide star adaptive optics system is presented. After the first light using natural guide stars with limited configuration of the system in October 2006, we concentrated to complete a final configuration for a natural guide star to serve AO188 to an open use observation. On sky test with full configurations using natural guide star started in August 2008, and opened to a public one month later. We continuously achieved around 0.6 to 0.7 of Strehl ratio at K band using a bright guide star around 9th to 10th magnitude in R band. We found an unexpectedly large wavefront error in our laser launching telescope. The modification to fix this large wavefront error was made and we resumed the characterization of a laser guide star in February 2009. Finally we obtained a round-shaped laser guide star, whose image size is about 1.2 to 1.6 arcsec under the typical seeing condition. We are in the final phase of commissioning. A diffraction limited image by our AO system using a laser guide star will be obtained in the end of 2010. An open use observation with laser guide star system will start in the middle of 2011.

**Keywords:** adaptive optics, laser guide star, curvature sensor, bimorph mirror, Subaru Telescope

## 1. INTRODUCTION

A curvature sensing technique is one of the most efficient AO system<sup>1</sup> The first generation AO system attached on Cassegrain focus of the Subaru Telescope, AO36,<sup>2</sup> has 36 elements curvature wavefront sensor and 36-elements bimorph deformable mirror. We decided to push forward the merit of this efficiency up to 188 elements of curvature sensing technique for a second generation AO system at Subaru Telescope.<sup>3,4</sup> Also a single sodium laser guide star system is incorporated to our second generation AO system to maximize the sky coverage.<sup>5</sup> The project of AO188 was funded in 2002. We got 5 years' budget for fabrication and construction of the system and consecutive 5 years' budget for commissioning and science program.

## 2. SYSTEM OVERVIEW

### 2.1 System layout

A new curvature AO system with 188 elements, AO188, is mounted at Nasmyth focus of the Subaru Telescope, instead of at Cassegrain focus. A facility instrument, the infrared camera and spectrograph, IRCS, which was formerly at Cassegrain focus with AO36, is modified to use at Nasmyth focus with AO188. A laser system needs clean and thermally stabilized environment to guarantee a stable operation in output power, beam quality, and

---

Further author information: (Send correspondence to Yutaka Hayano)  
Yutaka Hayano.: E-mail: hayano@subaru.naoj.org, Telephone: 1 808 934 5941

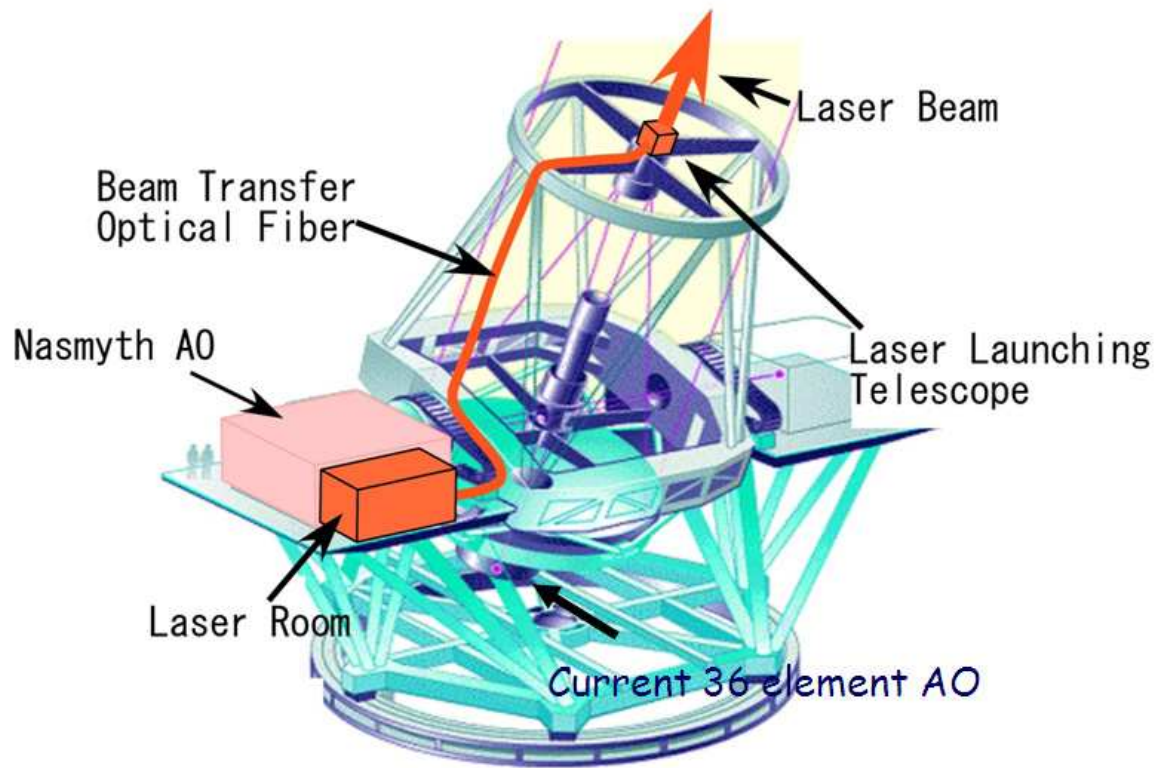


Figure 1. The layout of laser guide star AO system at Subaru Telescope. AO system and the laser are mounted on the Nasmyth platform. We mount the laser launching telescope behind the secondary mirror. The laser beam is transferred from the laser room to the laser launching telescope by the optical fiber.

oscillating wavelength. Thus, a thermally stabilized laser clean room is built at a stable Nasmyth platform. An optical fiber transfers a laser beam from the laser clean room to a laser launching telescope behind the secondary mirror of Subaru Telescope. While the optical fiber is installed permanently to Subaru Telescope, the laser launching telescope need to attach and detach for every demand of laser projection to the sky. Figure 1 shows a system layout to the Subaru Telescope.

## 2.2 AO system description

AO188 is mounted between Subaru Telescope and science instruments. There is no pick-off mirror, so that we need to moved away AO188 if science instruments do not want to use AO188.

Figure 2 shows a optical layout of AO188. AO188 receives  $f/13.9$  beam from the telescope. Field of view to science instruments is designed as 2 arcmin. The first optical component is a derotator (AO IMR in Figure 2), which can rotate the field on sky. We use three-mirrors system to change the orientation of the field on sky as well as the telescope pupil pattern. The off-axis parabola (OAP1 in Figure 2) collimates the beam and images the telescope pupil on the deformable mirror. The pupil size on the deformable mirror is 90 mm. Between the first off-axis parabola and deformable mirror, we insert an atmospheric dispersion collector (ADC in Figure 2). The ADC is designed to compensate an chromatic dispersion by atmosphere from visible to near infrared.<sup>6</sup> Deformable mirror with 188 elements<sup>7</sup> is mounted on a tip-tilt mount (DM/TT in Figure 2). Since the temporal bandwidth limit of the tip-tilt mount is quite limited, only averaged offset of tip-tilt on the deformable mirror

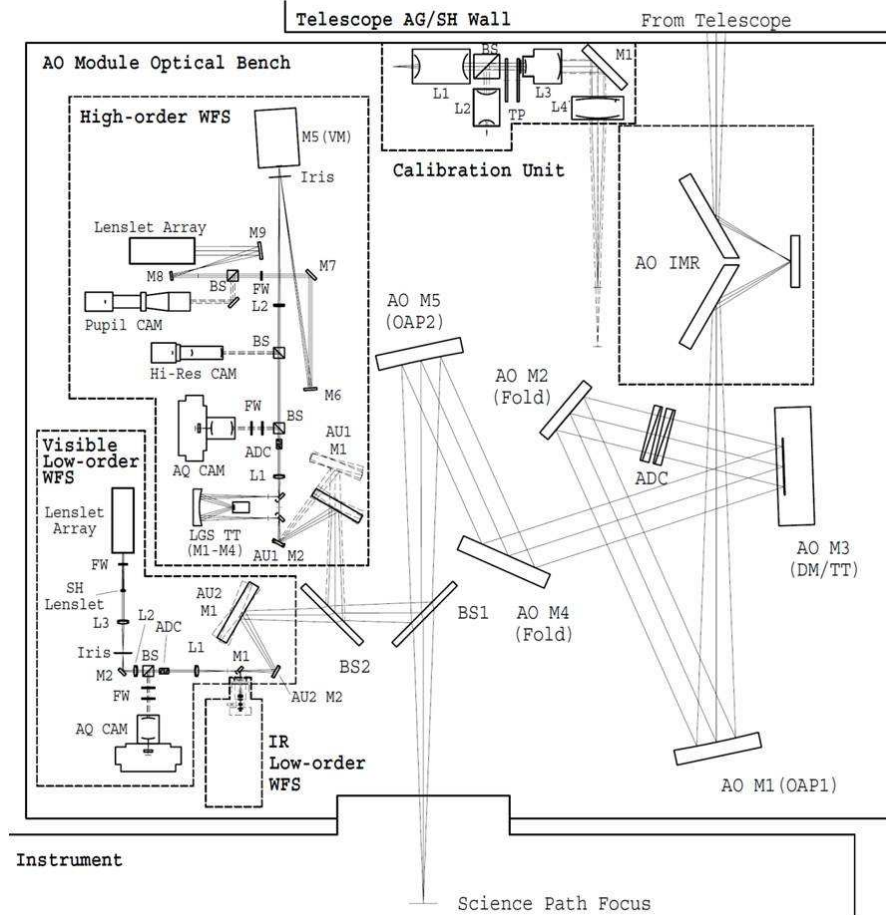


Figure 2. The optical layout of AO188.

is fed back to the tip-tilt mount. The stroke of each axis of tip-tilt mount is  $\pm 5$  arcsec. Offset on the tip-tilt mount is off-loaded to the telescope pointing. For the observation aimed in the thermal near infrared wavelength longer than  $2.5 \mu\text{m}$ , the offset on the tip-tilt mount shift a thermal background on the science detector. Thus we offload a tip-tilt offset on the deformable mirror directly to the telescope secondary mirror.<sup>8</sup> The second off-axis parabola (OAP2 in Figure 2) converges the beam again into focal ratio of 13.9.

Prior to science instruments, beamsplitters (BS1 in Figure 2) reflect a part of light for wavefront sensing. Three beamsplitters in total can be mounted to the automated exchange system. One beamsplitter reflects a visible light shorter than  $900 \text{ nm}$ .<sup>9</sup> Second one reflects shorter than about  $635 \text{ nm}$ , which is used for an optical science instruments. Third one is for an infrared wavefront sensor.

We have two wavefront sensors. One is a 188 sub-aperture curvature wavefront sensor as a high-order wavefront sensing and another is a  $2 \times 2$  sub-aperture Shack-Hartmann wavefront sensor as a low-order wavefront sensing, especially for tip-tilt and focus.

Another beamsplitter (BS2 in Figure 2), which is optimized to reflect a light from a sodium laser guide star, divides optical paths to two wavefront sensors. When we use only a natural guide star, a high-reflective mirror sends all light to the high-order wavefront sensor. We can switch between these two modes using automated exchange system.

A guide star is selected by a two-mirror system to wavefront sensors. We can select a guide star different from the science object within the  $2 \text{ arcmin}$  diameter field for the high-order wavefront sensor. (AU1 M1 and

AU1 M2 in Figure 2) The low-order wavefront sensor has a wider selectable field of view of searching a guide star at 2.7 arcmin. (AU2 M1 and AU2 M2 in Figure 2) Two-mirror system, worked as a guide star acquisition system, controls the position as well as the focus of science object on a science camera.

The field of view of the high-order wavefront sensor is 4 arcsec. We also use a field stop (Iris inside the high-order WFS in Figure 2) down to 1 arcsec to reduce a sky background and aliasing effect in curvature sensing. A vibrating mirror (VM inside the high-order WFS in Figure 2), placed at focal position, can moves back and forth of the position of telescope pupil on the 188-elements fixed lenslet array. The distance from the pupil plane to measure the curvature can be changed by the vibrating amplitude of the mirror. Light corrected by each lenslet array is injected to a large-core multi mode optical fibers and feeds to a photon counting APDs.<sup>10</sup> The geometry of electrodes on the deformable mirror and that of lenslets in the high-order wavefront sensor are well matched. Sampling rate of high-order wavefront is selectable. We use 1 kHz sampling typically.

The low-order wavefront sensor has 4 arcsec field of view, same as high-order wavefront sensor. We placed  $2 \times 2$ -element lenslet array at the position where the telescope pupil is conjugated, and  $4 \times 4$ -element lenslet array is located at the focal position of  $2 \times 2$ -element lenslet array, instead of putting a CCD array. Multi mode optical fibers are mounted exactly where the focal position of  $4 \times 4$ -element lenslet array. A photon counting APDs are also used to detect the light corrected by the  $4 \times 4$ -element lenslet array with optical fiber.<sup>11</sup>

### 2.3 Laser guide star system

A coherent light source at sodium resonance spectral line at 589 nm is generated by a sum-frequency mixing of two Nd:YAG laser at the wavelength of 1064 nm and 1319 nm.<sup>12,13</sup> Periodically poled MgO-doped stoichiometric lithium tantalate (PPMgO:SLT) crystal is used for sum-frequency generation. The average output power was started from 4.5 W in 2006 and finally it reached at 6.8 W after a fine tuning of laser system.<sup>14</sup> The laser is located in the thermally stabilized laser clean room. The room temperature is controlled at 22 degree Celsius. Stability of the room temperature is within 0.1 degree during the laser operation.

The laser beam is focused by a off-the-shelf doublet lens onto a solid-core photonic crystal fiber (PCF), whose mode field diameter is about  $14.3 \mu\text{m}$ . Both the doublet lens and the connector jacket of PCF are mounted on the 3-axis linear stages. The adjustment the position and the distance between the tip of the PCF and lens allows us to maximize the coupling efficiency. The maximum overall throughput of the optical fiber we achieved is about 75 %.<sup>15,16</sup> The laser launching telescope is mounted behind the secondary mirror of the telescope. The aperture size of the laser launching telescope is 500 mm, while the input aperture size is 40 mm. Thus this is a beam expander, whose magnification is 12.5. The telescope has three mirrors, primary, secondary and tertiary, similar to a bent Cassegrain telescope. We found that the wavefront error at the center area degrades the image quality at the sodium layer, which is caused by the stress at the connection between the primary center area and the tertiary support structure. Finally, the wavefront error within a full aperture is reduced by less than 100 nm after the modification of the mechanical structure.

The laser beam coming out from the PCF at the laser launching telescope is collimated by the lens. We chose the beam size about 25 mm. The steering of the laser beam is done by moving the lens laterally to the optical axis. The steering step is designed as 0.1 arcsec on sky. It is not necessary to steer a pointing direction of the launched beam in real time, since the position error of the laser guide star is compensated by the dedicated tip-tilt mirror inside the high-order wavefront sensor (LGS TT inside the high-order WFS in Figure 2). Tip-tilt offset on the dedicated tip-tilt mirror is offloaded by the position correction at the guide star acquisition system in front of the high-order wavefront sensor. The averaged focus error measured by the laser guide star indicates the estimation error of the mean altitude of the laser guide star. The offset of focus error is also compensated by the acquisition guide star unit. The rest of higher-order wavefront error is fed back to the deformable mirror.

## 3. OVERVIEW OF CURRENT STATUS

### 3.1 Performance using natural guide stars

We are monitoring the performance of AO188 using natural guide star since 2008. The Strehl ratio at K band for various brightness of guide stars are plotted in Figure 3. We achieved the Strehl ratio around 0.6 to 0.7 for the bright guide stars. The Strehl ratio is still larger than 0.2 even though the guide star magnitude is around

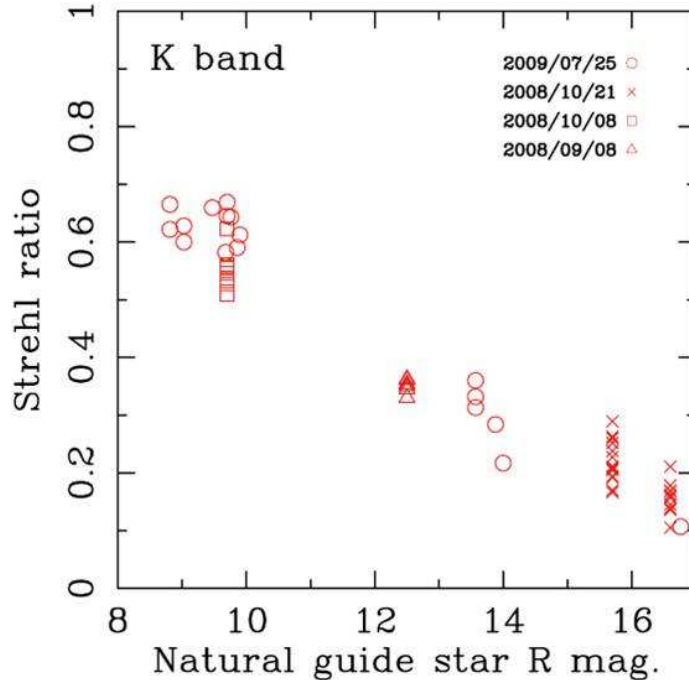


Figure 3. The estimated Strehl ratio as a function of the brightness of guide stars at K band, 2.2  $\mu\text{m}$ .

15 in R band. Sampling rate was 1 kHz for all cases from bright to faint guide stars. Since the photon-counting APDs have no readout noise, the performance using the fainter guide star was not apparently degraded.

The detail performance, including the isoplanatic angle and the Strehl ratio at other wavelength, is described in the other paper.<sup>17</sup>

### 3.2 On sky evaluation of laser guide star

Several engineering observations to create a laser guide star reveals that a typical image size in full width half maximum is around 1.2 to 1.6 arcsec at zenith under an averaged seeing condition. Figure 4 shows an example of a laser guide star image, taken by the CCD camera in the high-order wavefront sensor. The exposure time is 20 seconds. The brightness of a laser guide star at zenith was about equivalent magnitude of 10.7 in R band. We estimated that the laser power just after the launching telescope is around 4 W.

The brightness of a laser guide star as a function of elevation is also evaluated.<sup>14</sup> A simple geometrical model predicts that the brightness of a laser guide star decreases by air mass, because the brightness decreases as a square of a distance to a laser guide star, which is proportional to a square of air mass, and the brightness increases linearly of column length of sodium layer, which is proportional to air mass. Our measurement matched this model prediction approximately.

Also, the brightness change due to a wavelength offset was measured as well.<sup>18</sup> We found an unexpectedly wide tunable range, with which a laser guide star has enough brightness. Measuring a bandwidth of a laser beam relayed by the PCF, spectral broadening was found due to a self-phase modulation effect inside the PCF. This is caused by a high peak power in the PCF. While the initial spectral bandwidth of the laser is 1.7 GHz, the output laser after PCF has about 8 GHz. We roughly estimated that the efficiency of a return signal of sodium fluorescence light is degraded by a factor of 4 or 5.

### 3.3 Estimation of limiting magnitude of low-order wavefront sensor

We estimated the limiting magnitude of a low-order wavefront sensor. The averaged photo-counts of each APD at the low-order wavefront sensor for faint guide stars are plotted in Figure 5. Based on our experience of

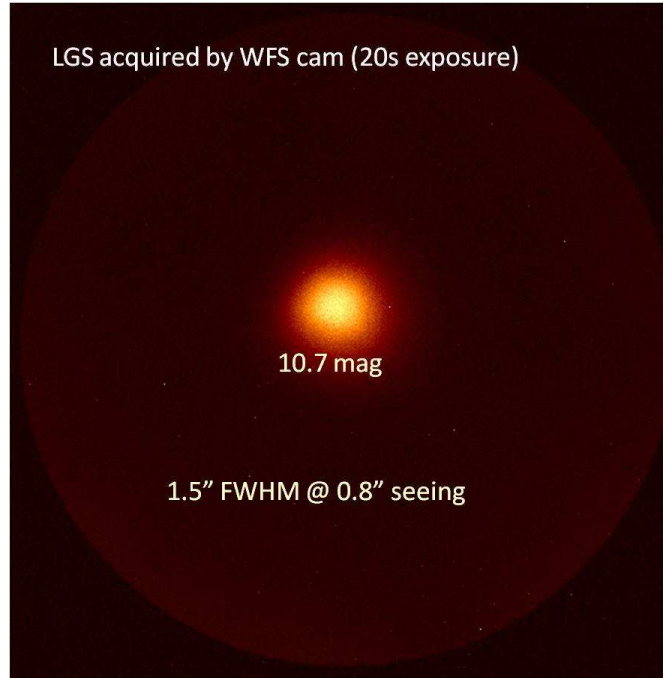


Figure 4. An image of laser guide star at zenith taken by the CCD camera in the high-order wavefront sensor. The brightness of the laser guide star is about equivalent magnitude of 10.7 in R band. The image size at the full width half maximum is 1.5 arcsec.

estimating a limiting magnitude of high-order wavefront sensor, We assume that a wavefront error in tip-tilt and focus can be measured at the photo-counts of APDs of 10 for each sampling rate at 100 Hz. Figure 5 indicates that the guide star at the magnitude around 18 in R band can be used as a tip-tilt and focus natural guide star. Unfortunately, we had a serious trouble in deformable mirror at this experiment, so that we could not evaluate the closed loop performance itself using the faint guide star.

#### 4. SCHEDULE OF COMMISSIONING

We are in the final phase of commissioning. Most components will be modified, integrated and tested by the end of October in 2010. The engineering observation and open use observation using natural guide star will resume in November, 2010. Seven nights in total for engineering observation have been assigned until the end of January, 2011. Performance evaluation of AO188 using a laser guide will be continued until the end of 2011. The risk-shared open use observation using a laser guide star will start during the final commissioning phase around in the middle of 2011. Finally, AO188 with a laser guide star will be served fully to open use observation in 2012.

#### 5. SUMMARY

The commissioning of the next generation AO for Subaru Telescope, AO188, is in the final phase. The AO188 system using a natural guide star has been served to open use observation since 2008. We achieved around 0.6 to 0.7 of Strehl ratio at K band using a bright guide star around 9th to 10th magnitude in R band. We succeeded to create a laser guide star in good quality. The image size is about 1.2 to 1.6 arcsec under the typical seeing condition. Final integration and testing is going on until October, 2010. Then we resume on sky evaluation through an engineering observation especially for using a laser guide star. After performance evaluation about one year in 2011, AO188 with a laser guide star will be served to risk-shared open use observation in the middle of 2011. Most of the risks will be reduced by 2012.

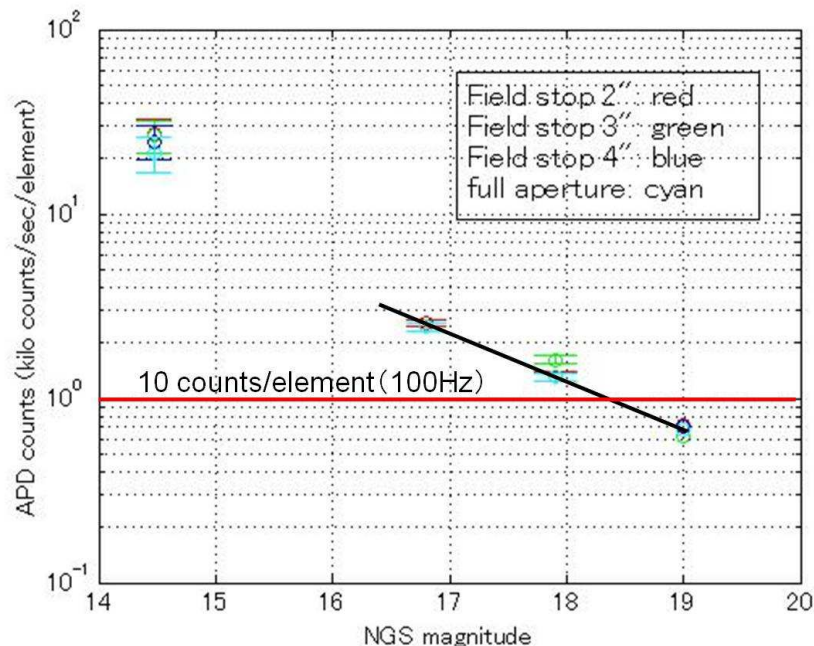


Figure 5. The average photo-counts of APDs as a function of natural guide star magnitude. We assume that a limiting magnitude, which can compensate a tip-tilt and focus wavefront error, corresponds to an averaged photo counts of 10 for each sampling rate at 100 Hz.

## ACKNOWLEDGMENTS

We thank our colleagues at the Subaru Telescope, especially the staffs, who supported us during an integration, daytime testing, and engineering observation of AO188 system at the summit of Mauna Kea. This work has been supported by Grant in aid of MEXT (Ministry of Education, Culture, Sports, Science and Technology) and Subaru Telescope, NAOJ.

## REFERENCES

- [1] Racine, R., “The Strehl efficiency of adaptive optics systems,” *PASP* **118**, 1066–1076 (2007).
- [2] Takami, H., Takato, N., Hayano, Y., Iye, M., Oya, S., Kamata, Y., Kanzawa, T., Minowa, Y., Otsubo, M., Nakashima, K., Gaessler, W., and Saint-Jacques, D., “Performance of Subaru Cassegrain adaptive optics system,” *PASJ* **56**, 225–234 (2004).
- [3] Takami, H., Colley, S., Dinkins, M., Eldred, M., Guyon, O., Golota, T., Hattori, M., Hayano, Y., Ito, M., Iye, M., Oya, S., Saito, Y., and Watanabe, M., “Status of Subaru laser guide star AO system,” *Proc. SPIE* **6272**, 62720C-1 – 62720C-10 (2006).
- [4] Hayano, Y., Takami, H., Guyon, O., Oya, S., Hattori, M., Saito, Y., Watanabe, M., Murakami, N., Minowa, Y., Ito, M., Colley, S., Eldred, M., Golota, T., Dinkins, M., Kashikawa, N., and Iye, M., “Current status of the laser guide star adaptive optics system for Subaru Telescope,” *Proc. SPIE* **7015**, 701510-1 – 701510-8 (2008).
- [5] Hayano, Y., Saito, Y., Ito, M., Saito, N., Kato, M., Akagawa, K., Takazawa, A., Colley, S., Dinkins, M., Eldred, M., Golota, T., Guyon, O., Hattori, M., Oya, S., Watanabe, M., Takami, H., Wada, S., and Iye, M., “The laser guide star facility for Subaru Telescope,” *Proc. SPIE* **6272**, 627247-1 – 627247-7 (2006).
- [6] Egner, S. E., Ikeda, Y., Watanabe, M., Hayano, Y., Golota, T. I., Hattori, M., Ito, M., Minowa, Y., Oya, S., Saito, Y., Takami, H., and Iye, M., “Atmospheric dispersion correction for the Subaru AO system,” *Proc. SPIE* **7736**, in press (2010).

- [7] Oya, S., Bouvier, A., Guyon, O., Watanabe, M., Hayano, Y., Takami, H., Iye, M., Hattori, M., Saito, Y., Ito, M., Colley, S., Dinkins, M., Eldred, M., and Golota, T. I., "Performance of the deformable mirror for Subaru LGS AO," *Proc. SPIE* **6272**, 62724S-1 – 62724S-8 (2006).
- [8] Oya, S., Hattori, M., Minowa, Y., Hayano, Y., Negishi, S., Tomono, D., Terada, H., Pyo, T. S., Watanabe, M., Ito, M., Saito, Y., Egner, S. E., Takami, H., Iye, M., Guyon, O., Garrel, V., Colley, S., and Golota, T. I., "Tip/tilt offload of Subaru AO188 by telescope secondary mirror," *Proc. SPIE* **7736**, in press (2010).
- [9] Minowa, Y., Takami, H., Watanabe, M., Hayano, Y., Miyake, M., Iye, M., Oya, S., Hattori, M., Murakami, N., Guyon, O., Saito, Y., Ito, M., Colley, S., Dinkins, M., Eldred, M., and Golota, T., "Development of a dichroic beam splitter for Subaru AO188," *Proc. SPIE* **7015**, 701561-1 – 701561-8 (2008).
- [10] Watanabe, M., Oya, S., Hayano, Y., Takami, H., Hattori, M., Minowa, Y., Saito, Y., Ito, M., Murakami, N., Iye, M., Guyon, O., Colley, S., Eldred, M., Golota, T., and Dinkins, M., "Implementation of 188-element curvature-based wavefront sensor and calibration source unit for the Subaru LGS AO system," *Proc. SPIE* **7015**, 701564-1 – 701564-8 (2008).
- [11] Watanabe, M., Ito, M., Oya, S., Hayano, Y., Minowa, Y., Hattori, M., Saito, Y., Egner, S. E., Takami, H., Iye, M., Guyon, O., Garrel, V., Colley, S., and Golota, T. I., "Visible low-order wavefront sensor for the Subaru LGS AO system," *Proc. SPIE* **7736**, in press (2010).
- [12] Saito, Y., Hayano, Y., Saito, Y., Ito, M., Saito, N., Kato, M., Akagawa, K., Takazawa, A., Colley, S., Dinkins, M., Eldred, M., Golota, T., Guyon, O., Hattori, M., Oya, S., Watanabe, M., Takami, H., Iye, M., and Wada, S., "589 nm sum-frequency generation laser for the LGS/AO of Subaru Telescope," *Proc. SPIE* **6272**, 627246-1 – 627246-7 (2006).
- [13] Saito, N., Akagawa, K., Ito, M., Takazawa, A., Hayano, Y., Saito, Y., Ito, M., Takami, H., Iye, M., and Wada, S., "Sodium  $D_2$  resonance radiation in single-pass sum-frequency generation with actively mode-locked Nd:YAG lasers," *Optics Letters* **32**, 1965–1967 (2007).
- [14] Saito, Y., Hayano, Y., Ito, M., Minowa, Y., Egner, S. E., Oya, S., Hattori, M. W. M., Garrel, V., Akagawa, K., Guyon, O., Colley, S., Golota, T. I., Saito, N., Takazawa, A., Ito, M., Takami, H., Wada, S., and Iye, M., "The performance of the laser guide star system for the Subaru Telescope," *Proc. SPIE* **7736**, in press (2010).
- [15] Ito, M., Hayano, Y., Saito, Y., Akagawa, K., Kato, M., Saito, Y., Takazawa, A., Takami, H., Iye, M., Wada, S., Colley, S., Dinkins, M., Eldred, M., Golota, T., Guyon, O., Hattori, M., Oya, S., and Watanabe, M., "Transmission characteristics of high-power 589-nm laser beam in photonic crystal fiber," *Proc. SPIE* **6272**, 627245-1 – 627245-8 (2006).
- [16] Ito, M., Hayano, Y., Saito, Y., Takami, H., Saito, N., Akagawa, K., Takazawa, A., Ito, M., Wada, S., and Iye, M., "High-power laser beam transfer through optical relay fibers for a laser guide adaptive optics system," *Publications of the Astronomical Society of Japan* **61**, 763 – 768 (2009).
- [17] Minowa, Y., Hayano, Y., Oya, S., Watanabe, M., Hattori, M., Guyon, O., Egner, S. E., Saito, Y., Ito, M., Iye, M., Takami, H., Garrel, V., Colley, S., and Golota, T. I., "Performance of Subaru adaptive optics system AO188," *Proc. SPIE* **7736**, in press (2010).
- [18] Ito, M. et al., "The characteristics of laser-transmission and guide star's brightness for Subaru LGS/AO188 system," *Proc. SPIE* **7736**, in press (2010).